

SmallSat Platform Development for Coast Guard Academy Collaborative Space-Based Research

Royce W. James
US Coast Guard Academy/US Air Force Institute of Technology
2950 Hobson Way, ENP, Wright Pat Air Force Base, OH, 45433; 937.255.6565 x4339
Royce.W.James@uscga.edu

Richard W. Freeman, Lorraine A. Allen
US Coast Guard Academy; 860.444.8533
15 Mohegan Ave, New London, CT 06320
Richard.W.Freeman@uscga.edu; Lorraine.A.Allen@uscga.edu

Erik Tejero
US Naval Research Laboratory, Plasma Physics Division
4555 Overlook Ave SW, Washington, DC 20375; 202.767.3215
Erik.Tejero@nrl.navy.mil

Brian Kay
US Air Force Institute of Technology
2950 Hobson Way, ENP, Wright Pat Air Force Base OH, 45433; 937.255.6565
Brian.Kay@afit.edu

Jin S. Kang,
US Naval Academy
121 Blake Road, Annapolis, MD 21402; 410.293.6411
Kang@usna.edu

ABSTRACT

Collaborations utilizing small spacecraft in near earth orbit between the U. S. Coast Guard Academy (CGA), Naval Research Lab (NRL), the U. S. Naval Academy (USNA), and the Air Force Institute of Technology (AFIT) have initiated scientific and engineering space -based experiments. Sourced opportunities like the VaSpace ThinSat missions have provided a platform for payload, sensor, and experiment development that would have otherwise been resource prohibitive. We have constructed an impedance probe payload for launch in Fall 2020 derived from the existing 'Space Plasma Diagnostic suite' (SPADE) mission operating from NASA's International Space Station. Currently both space and laboratory plasmas are investigated with AC impedance measurements using a radio frequency antenna. Plasma electron density data collected from the ThinSat will however use an innovative surface-mounted dipole antenna to gather the required sheath-plasma and plasma resonance information. On that same launch, a compact multispectral 'Pixel Sensor' with a 450 nm – 1000 nm spectral range will add to the existing Inertial Motion Unit, Temperature Sensor, Infrared Sensor, and Energetic Particle Detector baselined in previous launches. Our engineering team has begun to design, build, and test a solar panel deployment and de-orbiting mechanism for a CubeSat with the USNA's Aerospace Engineering Department that utilizes a miniature motor for deployment actuation. For the motor to produce the required torque, a gear ratio of 20:1 is necessary. Impedance probe optimization, de-orbiting mechanism automation, and data collection obstacles, solutions, and procedures will be reported.

INTRODUCTION

Scientific and Engineering discovery and development is integral to the development and continuance of Military Science past, present, and future. Science and Engineering challenges have been conceived, framed, and overcome by Military Scientists for centuries and will continue to be in the future. Preparing our future Officers, Technicians, and Civil Servants to carry the torch of discovery and meet our future missions is vital. Our U. S. Coast Guard Academy (USCGA), Naval

Research Lab (NRL), the U. S. Naval Academy (USNA), and the Air Force Institute of Technology (AFIT) small spacecraft in near earth orbit collaboration has devised scientific and engineering space-based experiments and payloads. Our research is in direct support of NASA ISS missions, Coast Guard and USCGA Remote Sensing Science Research and eventually novel ideas like SmallSat intra-cluster laser communications. At the Coast Guard Academy Plasma Lab (CGAPL), USCGA space initiatives in partnership with our collaborators have developed two SmallSats, a ThinSat and a

ThickSat. Each spacecraft has its own payload, an impedance probe to make direct density measurements of space plasmas using a surface-mounted dipole antenna, a visual to near infrared sensor, and several standard sensors provided by the Virginia Commercial Space Flight Authority (VaSpace).

IMPEDANCE PROBE (IP) ONBOARD THE THICKSAT

Plasma parameter measurements are a key aspect of remote sensing terrestrial and space events from the upper atmosphere and low earth orbit (LEO). Deployable and orbital assets that gather in-situ data over long timescales (days to years) are invaluable references for observational data gathered in connection with specific events. It is especially lucrative to establish agile hardware and deployment vehicles that can accommodate multiple remote sensing architectures and sensors that are specific to the detection needs within this larger data collection umbrella. Ideally, a combined scenario of long-term established data, shorter-term targeted data, and real-time situational data could provide ample resolution with fidelity. USCGA then provide long-term established, shorter-term targeted, and real-time situational data to our partners and collaborators like AFIT and Naval Post Graduate School's (NPS) Atmosense data access collaboration, NRL's SPADE and United States Air Force Academy's (USAFA) Integrated Miniaturized Electrostatic Analyzer (iMESA) NASA ISS missions, while continuing to support our very own CGAPL and Science Department Remote Sensing courses and research.

Currently both space and laboratory plasmas are investigated with AC impedance measurements using a radio frequency antenna. Plasma electron density data collected from the ThinSat will, however, use an innovative surface-mounted dipole antenna to gather the required plasma sheath and resonance information. Spacecraft charging, plus ambient plasma temperature and density measurements are subsequently determined from the resonant impedance frequencies. Measurements are then converted from digital to analog values and processed for transmission through the ThinSat bus and gathered in both LEO plus during payload sensor and platform tests at low altitude (less than 1 km) and high altitude (~26 km).

Visual+NIR Sensor (VIR-S)

Since targets each possess a unique spectral signature, multispectral sensing allows characterization of objects within the field of view (FOV) if given reflectance values spanning a sufficient range of wavelengths. The Pixelteq's VIS+NIR multispectral PixelSensor array, containing eight (approximately) 3 mm x 3 mm pixels,

each registering a given wavelength band, is on board both the ThinSat and ThickSat. A lens with an 8 mm focal length gathers and focuses light on the PixelSensor. Calculation estimates a ground sampling distance of ~75 to 94 km from perigee (~200 km) to apogee (~250 km). Even so, large areas of snow, ice, water, desert, and vegetation, for example, dominating the field of view should be identifiable from the data through comparison with digital libraries of known spectral signatures, such

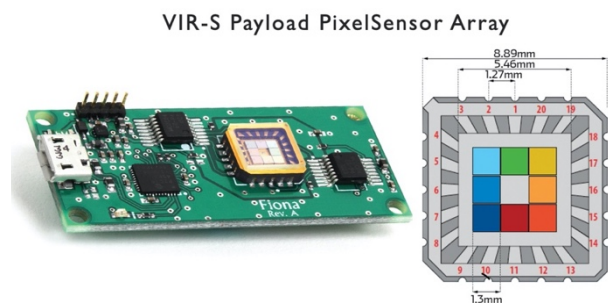


Figure 1 Pixelteq's multispectral array and original equipment manufacturer (OEM) electronics board. Photodiode coatings and specifically programmed OEM electronics provide narrow band selections into the near infrared wavelengths. Picture courtesy of pixelteq.com.

as provided by USGS. It may be possible to identify multiple targets within a given view, depending on the size and contribution of each target to the total recorded spectrum. Imagery of the FOV, such as from LandSat or other satellite data, is essential to corroborate the findings. Onboard the ThinSat is the PixelSensor without a lens, with a ~180° FOV; its data can be compared with that from the ThickSat and used to validate the orientation of the satellites and the identified targets in view.

Characterizing targets within the sensor's FOV will provide a valuable educational experience for students. It is hoped that differentiation within a given target class, such as variations in snow or ice (i.e., fresh, glacial, first-year), vegetation (i.e., healthy, stressed, grassland, forest), soil, sand, and water, for example, is possible from the data. Knowledge gained from the current mission is vitally important in validating the procedures and methods employed, such as sensor selection and mounting, and providing a baseline for future CGA passive space-based land, ice and water sensors; lessons learned will help steer the creation of future SmallSats (Thin/Thick/CubeSats) which serve Coast Guard missions, CGA's educational program and academic research.

The Ocean Insight VIS/NIR PixelSensor was chosen as the multispectral sensor. It has eight wavelength-

selective photodiodes that have center wavelengths between 400 and 1000 nm in a 9 mm x 9 mm sensor package. The width of each color band is 10 nm. The imager is only 41.7 mm x 21.4 mm x 1.5 mm. This compact design is an ideal size for the ThickSat and ThinSat payloads. Each photodiode produces 1 Byte of data. The data represents the light intensity of one discrete color band. The eight bytes in total, represent the spectrum.

The VIS/NIR PixelSensor has an operating voltage of 5V. The PixelSensor is designed for testing and evaluation using its microUSB connector and Arduino Integrated Development Environment. The sensor communicates using the I2C protocol. I2C is a synchronous, serial data communications protocol that operates using a four-wire bus, with, Power (5V), Ground, Serial Data (SDA) and Serial Clock (SCL).

ThinSat and ThickSat Payload Specifications

USCGA will deploy two SmallSats on the next Antares NG-15 mission, one ThinSat and a another SmallSat that is twice the thickness with the same footprint that we classify as a ThickSat. VaSpace has a standard suite of diagnostics available for deployment. In 2019, we deployed 3 ThinSats with these sensors as part of the NG-11 mission along with over 50 other investigation teams from NASA, planetariums, colleges, universities, service academies, and high schools across the nation. Each standard NearSpace Launch (NSL) sensor suite includes an available Energetic Particle Detector, Plasma Probe (electron plasma density), Infrared Sensor (radiated temperature), Temperature Sensor (onboard temperature), and a Inertial Motion Unit (3 axis accelerometer, magnetometer, gyrometer) if chosen by the investigation team. All three USCGA ThinSats from NG-11 carried the full suite of NSL sensors.

Comparable LEO data collected with the standard NSL sensors onboard the ThinSat will be compared to historical NG-11 data. Additionally, a single Pixelteq VIS+NIR multispectral PixelSensor will be added to the ThinSat payload compliment. Unfortunately, the ThinSat does not provide enough distance between the sensor surface and a mounted lens. Reduced resolution will absolutely occur at the earth's surface without the lens. Section 3 will describe in more detail important orientation and spectral data that will be obtained from this unresolved source.

Only two sensors will fly onboard as the ThickSat payload. USCGA merged two ThinSats along the length and height edges (see fig. 2) which creates an increased depth to accommodate the Lens' focal length and sensor integrated circuit PCB mounting. Lastly, the Impedance Probe (IP) with its surface mount antenna is the only other sensor onboard the ThickSat. We will discuss the

hardware, engineering, and physics associated with the IP in later sections. It is important to note that the surface mounted antenna also benefits from the extended width of the ThickSat to 25 mm for best positioning at the furthest possible separation.

Impedance Measurement Concept

The ThickSat's surface mounted dipole is designed to provide spacecraft charging and ambient plasma parameter measurements based on the modifications to

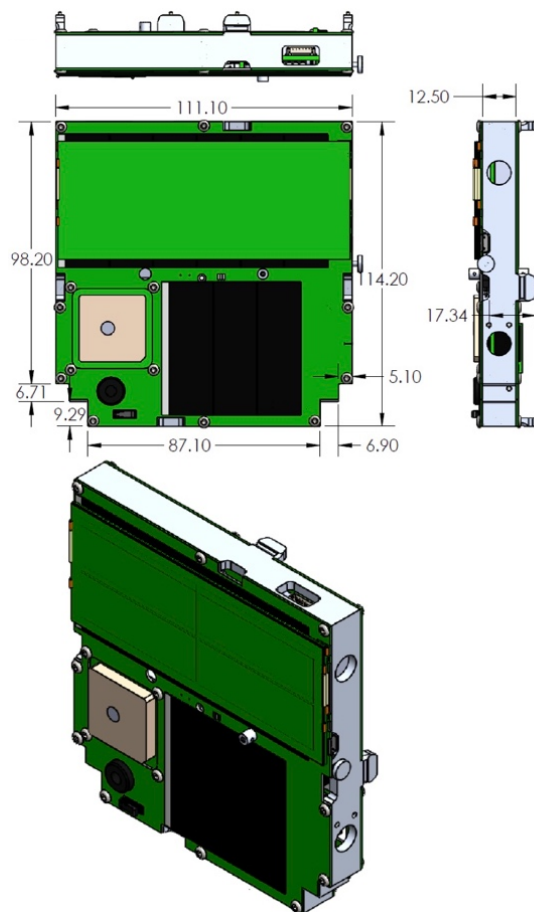


Figure 2 ThinSat External Dimensions. Courtesy of VaSpace (courtesy of NearSpace Launch Inc.).

ThickSat footprint dimensions are the same as the ThinSats but double the thickness, 25mm (ThickSat) versus 12.5mm (ThinSat).

the free space impedance of the dipole when immersed in a plasma. The probe will make measurements of the impedance of the plasma antenna system, which exhibits resonances at the sheath resonance and at the upper hybrid frequency.⁴ The impedance probe will make use of an RF-IV measurement circuit, which uses impedance matched radio frequency (rf) transformers to pick off voltage signals proportional to the rf voltage and rf

current in the antenna/plasma circuit. These signals are mixed with a local oscillator signal with a 0 and 90 degree phase shift to get the in-phase and quadrature components of both the rf voltage and current at the driver frequency. The rf voltage to rf current ratio will provide the impedance. The driver frequency is scanned to determine the impedance spectrum.

The expected impedance spectrum of a spherical probe in an unmagnetized plasma can be visualized as a tank circuit as in ref [1] with C_{sh} as the sheath capacitance created between the plasma and the vacuum chamber walls. Here we take Z to be

$$Z = \frac{1}{j\omega C_{sh}} + \frac{1}{j\omega C_0 + \frac{1}{R_p + j\omega L_p}} \quad (1)$$

with a collision frequency ν and plasma frequency ω_{pe} , and aspects of the plasma represented as circuit elements²

$$C_0 = 4\pi\epsilon_0\rho, \quad (2)$$

$$L_p = \omega_{pe}^{-2} C_0^{-1}, \quad (3)$$

$$R = \nu L_p. \quad (4)$$

Equation 1 has two resulting resonance points (series and parallel) for the impedance where the reactance is zero in frequency space

$$\omega_1 = \omega_{pe} \sqrt{\frac{C_0}{C_{sh} + C_0}} \quad (5)$$

$$\omega_2 = \omega_{pe} \quad (6)$$

where ω_1 is the series resonance and ω_2 parallel. Series resonance corresponds to the lowest reflected signal and maximum energy deposited into the plasma and is the more prominent in many measurement techniques.

At the resonant frequency the imaginary part of impedance goes to zero and the total impedance will be at a minimum. This is represented by a zero crossing of the phase. An impedance match between the ThickSat and the background plasma provides an excellent way to measure electron density. When the measured phase crosses zero, the resonant frequency is equal to the plasma frequency. When the frequencies match, we can solve for the plasma density, n_0

$$\omega_{pe} = \left(\frac{n_0 e^2}{\epsilon_0 m}\right)^{1/2} \quad (7)$$

where equation 4 describes the plasma frequency as a function density n_0 . Here lies the last major intellectual step in the impedance density relationship. Reflected power is monitored but the spectrum analyzer and can track the power deposited into the plasma by will be calculated from the resonance points in equation 3.⁴

Once the spacecraft is immersed in the plasma, a sheath will form around the antenna. The sheath will either be electron rich or depleted of electrons depending on the plasma potential between the ThickSats and the background plasma.

Two primary options are available in collecting spacecraft charging data with the impedance probe, positively or negatively biasing the probe antenna. If the probe is negatively biased compared to the plasma then a depleted electron (ion) sheath will form of thickness of

$$S(\phi) = \left(2 \cdot 5 - 1.87 e^{(-0.39 \frac{\rho}{\lambda_D})}\right) \left(\frac{e\phi}{KT_e}\right)^{\frac{2}{5}} \lambda_D. \quad (8)$$

$S(\phi)$ is a modified form of the Child-Langmuir Law where ϕ is the sheath thickness as a function of the electric potential, ρ is the sphere's radius, and λ_D is the Debye Length. The sheath plasma resonance noted by the first zero phase crossing in figure 3 represents a maximum power disposition associated with the series resonance, and ω_1 on this normalized frequency versus

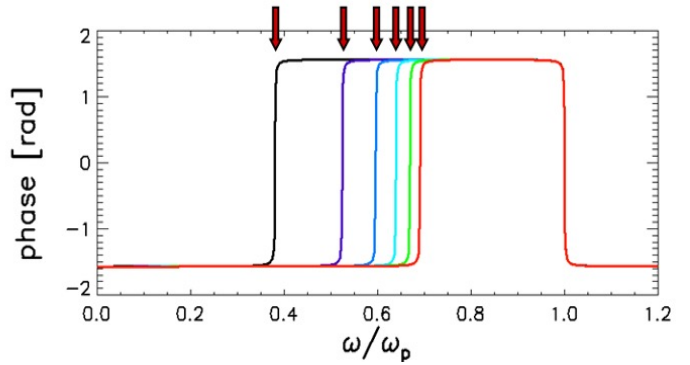


Figure 3 Phase of probe-plasma impedance used to determine the resonant frequencies for a spherical probe (theoretical data).⁶

phase plot. Impedance in-full is calculated by inserting the equation (8) into equation (1).

If the probe is positively biased then the sheath will have an excess number of electrons and form an electron rich sheath. At that point, Impedance can no longer be considered a capacitance and an extremely complicated

analytical approach is needed. A perturbation solution to Llewellyn's equation,

$$J(t) = \varepsilon_0 \frac{m}{e} \frac{\partial^3 x}{\partial t^3} \quad (9)$$

is used as an approximation to determine the impedance.² Integration of the AC electric field as function of the perturbed transit time acceleration over the entire sheath is required to determine its impedance. Each of the variables and steps are specified in reference 2,

$$Z^+(\beta, T) = \frac{T^2}{2\beta} \left[1 - \frac{\zeta}{3} \left(1 - \frac{12S(\beta)}{\beta^3} \right) \right] \frac{(v_{e0} + v_e)}{4\pi\varepsilon_0\rho^2} \quad (10)$$

however, the complete impedance is a combination of the sheath's and the plasma,

$$Z = Z^+(\beta, T) + \frac{1}{j\omega C_{sh}} + \frac{1}{j\omega C_0 + \frac{1}{R_p + j\omega L_p}} \quad (11)$$

DC Impedance Measurement is Untenable

A standard diagnostic method used to measure plasma parameters is to use DC source to step through DC bias voltages and measure the collected current at each step. Sheath capacitance is dependent on sheath thickness. Sheath capacitance is dependent on sheath thickness. Applying a DC bias enables us to control type of sheath that forms and its thickness. Being able to control the sheath capacitance we can tune the resonant frequency to find the impedance match. Due to size limitations and power budget constraints our ThickSats will not include a DC source. By not including a DC source we exclude a Langmuir probe and cannot measure electron temperature. However, our second ThickSat has a full suite of sensors and is capable of measuring electron temperature.^{4, 5, 7, 13}

AC Impedance Measurement Concept is Attainable

The ThickSats will make AC impedance measurements of the plasma using a surface-mounted dipole antenna. It will sweep through AC frequencies measuring time-dependent current and voltage until a resonant frequency is found. The resonant frequencies are when the impedance of the antenna is real and we observe a zero crossing of the phase. The phase flip is indicative of an impedance match, which gives us the plasma frequency. Analysis of the plasma frequency yields plasma density.⁴

Time-dependent current and voltage measurements from a Dipole antenna produces an altered impedance measurement in comparison to the spherical paradigm. Impedance is still the sum of the sheath and bulk plasma impedance slightly augmented due to the geometry of the short dipole wires:

$$Z = Z_{plasma} + Z_{sheath} = Z(\beta_p, L') + Z(\beta, L) - Z(\beta_s, L). \quad (12)$$

However, for the ThickSats metal surface mounted strips are used versus wire cylinders with different geometries and slightly different electromagnetic properties that affect the impedance. Some key differences are in the

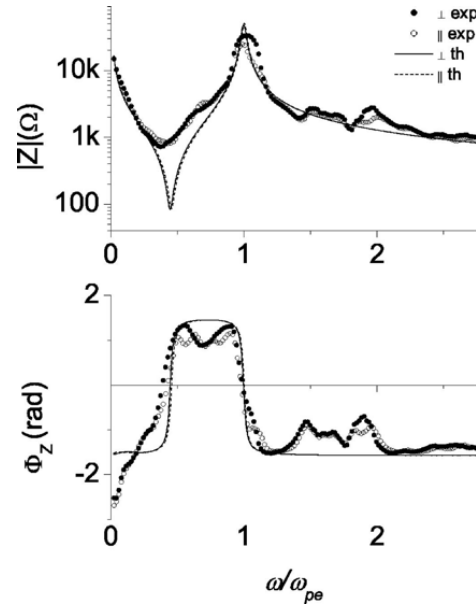


Figure 4 AC experimental and theoretical phase and impedance as a function of normalized frequency.

analytic solution to the perturbation which now results in

$$Z(\beta, L) = \frac{F(\beta)}{j\omega\pi\varepsilon_0 L} \quad (13)$$

where

$$F(\beta) = \ln \frac{(1 + \sqrt{1 + \beta^2})^2}{\beta(2 + \sqrt{4 + \beta^2})^2} \frac{1}{2} [3\beta + \sqrt{4 + \beta^2} - 4\sqrt{1 + \beta^2}] \quad (14)$$

and

$$\beta = \frac{\text{width}}{2L}. \quad (15)$$

With the surface mounted antenna impedance measurement, we will determine plasma density in the vicinity of the metal antenna strips. These strips are placed as far away from each other as possible on the ThickSat's 5.10 mm long sides, to maximize accuracy.

IP Hardware

At the Coast Guard Academy Plasma Lab (CGAPL), USCGA space initiatives in partnership with the Naval Research Lab have required the development of a ThinSat impedance probe to make direct temperature and density measurements of space plasmas using a surface-mounted dipole antenna. The roughly 10 cm x 10 cm x 2 cm payload platform is modified from the ThinSat platform provided by Virginia Commercial Space Flight Authority (Virginia Space) through a partnership with USCGA. An onboard 75 MHz Direct Digital Synthesizer (DDS) is used to sweep the AC frequency applied to the dipole where time-dependent current and voltage measurements are recorded. Additionally, a co-aligned 400-2500 nm hyperspectral sensor, LiDAR, and thermal camera package (amongst other sensor options) will be integrated onto a UAV for tactical deployment.

THINSAT AND THICKSAT PAYLOAD SPECIFICATIONS

The ThickSat uses the same bus as the standard ThinSat, so power, telemetry and communications are provided through it. ThinSats are designed to use sensor board This board connects to the bus and captures light intensity, temperature and pressure. The data is communicated through the bus, packetized and broadcast back to Earth over the 5-day life of the ThinSat mission.

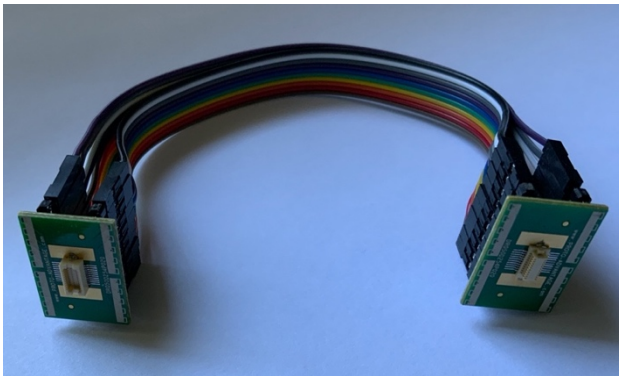


Figure 5 Prototype extension Cable for Impedance Probe

The modified ThickSat payload is comprised of the PixelSensor and Impedance Probe. The Impedance Probe connects into the bus using the same connector as the TSLBD circuitboard. The connector is surface-mounted and snap-fits to the bus. In a normal ThinSat, the bus and sensors are within a few millimeters of each other. The ThickSat was approved to accommodate the larger payload, but also created a situation in which the bus and sensor board are a few centimeters apart. The team designed a cable with connectors to connect the sensor and bus (figure 5).

ThickSat Circuit Replaces Standard Primary Board

As mentioned in above, the Impedance Probe will produce both AC and DC voltages and currents. While the Impedance Probe components can produce and transmit positive and negative voltages and currents, the Arduino Pro Mini is not capable of reading negative voltages and currents. Reading a negative voltage or current can damage the Analog-to-Digital Converter (ADC) on the Arduino and potentially damage the AT328MEGA processor in the Arduino. Since the Arduino is mission-critical, eliminating potential problems is important.

There are two potential solutions to avoid presenting a negative voltage to the Arduino- a level shifter or a subsystem that only presents positive voltages to the Arduino. The idea of a level shifter is to use electronics to shift (bias) voltage higher or lower. The Impedance Probe will produce voltages between -3 V and +3 V, and the Arduino Pro Mini has a maximum voltage of 3.3 V. You cannot shift the voltage level lower than 0 V, and you cannot shift the level higher than the maximum voltage output from the Arduino. Given these conditions, the team is either forced to modify the voltage range output from the AD9834s or use a different solution for eliminating negative inputs into the Arduino.

The second method investigated was creating a subcircuit using Comparators, Invertors and Multiplexers. This subcircuit compares the output of the AD9834 to Ground and inverts the output. If the output of the AD9834 is less than Ground, then the inverted output is passed through a 2:1 Multiplexer to the Arduino. If the output of the AD9834 is positive, it is passed through the 2:1 Multiplexer to the Arduino. The Comparator and Invertors are built using LM398 Operational Amplifiers (Op Amps). The initial tests were done with LM741 Op Amps. The LM741 is a general-purpose Op Amp that has heavy use in designs. This Op Amp needs 5V to operate. Since the Impedance Probe operates at 3.3V, the LM741 would require a 5 V line to it, or a Voltage Divider would be necessary to provide 3.3 V to the rest of the Impedance Probe. The LM398n is a low power Op Amp that operates at 3.3 V. The LM398n, in testing, proved to be a better choice. A single dual dip LM398n package provides two Op Amps which are required to create the Comparator and Invertor for the subcircuit, required for each output.

As the AD9834 DDS is a signal generator. As the DDS-generated signal interacts with the Plasma, the response is received by the antenna. The 1:1 Transformers are used to measure the current and voltage of the signal

response. Using 1:1 transformers attenuates transient noise with very little signal loss. With voltage limitations in the processor, it becomes very important to limit losses in transforming signal current to voltage.

Biasing the signal presents an interesting challenge. The acceptable input voltage range for the Arduino Pro Mini is 0 – 3.3 V. We can correct for the voltage bias with a series capacitor. While this reduces the output voltage, we can map the reduced output voltage to a higher known value.

VIR-S Requirement Modifications

The team determined there was an opportunity to use the PixelSensor as the payload on the ThinSat. This payload will include an 8mm optical lens, as discussed in 2.1. The PixelSensor’s power requirements fall under the power limits of the ThinSat. The PixelSensor draws a maximum of 0.5 W at 5 V. The importance of this is discussed in the next section, on the power budget.

The ThinSat has only a few places where optical sensors can be positioned. The bottom of the ThinSat has an opening for the Earth Sensor. This location cannot be used because the PixelSensor would have to face towards the bus, and there is not enough room to connect the sensor to the bus in this position. In addition, the Earth Sensor port is too large and the lens could fall through this port. There are also two circular ports for the Lux sensor that are located along the side of the ThinSat. At 12.5 mm thick, the ThinSat is too thin to position the PixelSensor board on its side and use one of these ports. The ports are in the wrong position for this use. The only port in a viable position is on top of the ThinSat, located under a solar panel. When the ThinSat is activated, and solar panel deployed, this port will be uncovered and usable for imaging. The solar panel will act as a lens cover, protecting the lens during launch. There are two potential problems with using this port- 1) failure of the solar panel to deploy and 2) the solar panel blocks imaging of the Earth.^{7, 13}

The solar panel can fail in two ways. The first potential solar panel is a failure with the burn wire. The burn wire must release the solar panel, which has a series of hinges and small panels that should open fully. If the burn wire fails, then the imager is blocked. The second potential solar panel failure is the panel blocking the imager’s field of view. Because we are chosen this port, the field of view is going to be partially blocked by the solar panel. The real problem is if the panel obscures the view of Earth. With the ThinSat, we have not ADCS or method of repositioning the satellite and accept there is a chance that the ThinSat will not be in position for imaging the Earth. The potential problem is If the satellite is position

for imaging and the solar panel blocks the view of Earth. There is also the opportunity to add the PixelSensor to a CubeSat to be launched on NG-16 in late 2021.

ThickSat Power Budget Limits

The ThickSat bus supplies 3.3 V and 5 V, with a maximum current of 0.100 A per line. The initial ThickSat payload power budget was computed as 0.6 W- 0.12 A @ 5 V, which, according to the ThinSat designer, Twiggs Space Lab, could potentially disable the bus if both sensors drew more than a total of 0.100 A, on the same 5 V line. There is no guarantee that the payload would not draw more than the maximum allowed current when the ThickSat bus activates during launch. To avoid potentially disabling the ThickSat on launch, another way of connecting the sensors to the bus was required. The Impedance Probe can operate at either 3.3V or 5V and communicates using the SPI Protocol. By connecting the Impedance Probe to the bus via the SPI pins on the bus and connecting the PixelSensor to the bus via the I2C pins, the team was able to reduce the power budget to 0.5 W on the 5 V line and 0.33 W on the 3.3 V line.

Table 1 Impedance Probe (top) and VIR-S Multispectral Sensor (bottom) power budget for the ThickSat.

| Description | Part # | Voltage (V) | Current (A) | Power (W) |
|---------------------------|-----------------|-----------------|-------------|-----------|
| CPU - 8MHz | Atmega328p | 3.3 | 0.014 | 0.045 |
| DDS | AD9834 (2) | 3.3 | 0.012 | .04 |
| DDS | AD9834 (2) | 3.3 | 0.006 | 0.0201 |
| 72 MHz CLK | SG-210STF | 3.3 | 0.003 | .0099 |
| Signal Sel OPAMP | LM358 (4) | 3.3 | 0.0005 | 0.0016 |
| Multiplexer | SN74HC74DE 4 | 3.3 | 0.024 | 0.08 |
| IP Power Budget | | Total Required: | 0.0595 A | 0.1966 W |
| Description | Part # | Voltage (V) | Current (A) | Power (W) |
| Multi Spec Sensor | OEM | 75 | 0.0002 | N/A |
| High Volt Op Amp | OPA454 | 5 | 0.05 | 0.25 |
| VIR-S Power Budget | | Total Required: | 0.0502 A | 0.25 W |

SOLAR DEORBITING FOR FUTURE CUBESAT

There are other nano and pico-satellite activities at USCGA. One of our interdisciplinary capstone teams in Electrical and Mechanical Engineering designed and built a Solar Panel deployment system to position solar panels and deorbit a 2U CubeSat. This was a joint project with USNA’s Aerospace Engineering Department. There were two major design questions that needed to be answered- 1) what method could be used to move the solar panels on demand and hold position, and 2) could that method use motors even though satellite batteries will be near their end-of-life after five years in space?

The capstone team was able to design a system that used a single motor and gear set to control the movement of four solar panels. An analysis of the battery capacity at five years revealed that approximately 14% of battery capacity would be available. The team designed for a motor that would require only 0.06% of the battery's remaining power to move the solar panels from the operational position of 135° to the deorbit position of



Figure 6 3U CubeSat with Solar Panels deployed¹⁹

90°. The repositioning of the solar panels is calculated to take 30 seconds. Moving the solar panels to 90° will increase atmospheric drag on the CubeSat and cause it to deorbit. The team had to research and develop strategies to address, corrosion, cold welding and positioning. This design will be completed and tested over the next several months and is scheduled for launch on NG-16 during the Fall of 2021.

CONCLUSION

At mission completion, the team will measure plasma densities in the $n_e \sim 10^2 \text{ cm}^{-3}$ or greater in LEO plus detect reflected and emissive terrestrial light. Success is firmly based on gathering the density and visual data from both spacecraft. Fidelity will be determined with ISS plasma data from SPADE and iMESA over similar spatial and relative near time periods.

Experiments to minimize size and power requirements by implementing a single motor to control the movement of all four solar panels with a gear train assembly to move all panels will minimize motor size and power budget. The motor will be mounted near the center of the CubeSat and will drive a worm gear mechanism to simultaneously move all the solar panels at the same position. This system will be installed into a 1.5 U CubeSat and launched Late Spring/Early Summer of 2020. The motor used in the assembly requires 3 V and 0.15 A to produce a torque of 0.039 Newton-meters (Nm). The motor operates at 15 RPM at this power. Lower power can be used to drive the motor, resulting in

decreased speed and time to reposition. At 15 RPM, the motor takes 30 seconds to rotate from the original starting position into the desired position of 135°. It requires 13.5 J of energy during this time. This position change requires 0.0028 W to operate, which is 0.06% percent of the original battery capacity.

Plasma parameter measurements are a key aspect of remote sensing terrestrial and space events from the upper atmosphere and low earth orbit (LEO). Deployable and orbital assets that gather in-situ data over long timescales (days to years) are invaluable references for observational data gathered in connection with specific events. It is especially lucrative to establish agile hardware and deployment vehicles that can accommodate multiple remote sensing architectures and sensors that are specific to the detection needs within this larger data collection umbrella. Ideally, a combined scenario of long-term established data, shorter-term targeted data, and real-time situational data could provide ample resolution with fidelity. Future research and missions will focus on meeting these objectives.

Acknowledgments

We acknowledge support by U.S. DEPS Grant [DE-JTO] PRWJFY19. Dr. Tejero was supported by the NRL base program.

References

1. Akiyama H., "Streamer discharges in liquids and their applications," IEEE Transactions on Dielectrics and Electrical Insulation, vol. 7, Issue 5, October 2000.
2. D. D. Blackwell, D. N. Walker, S. Messer, and W. E. Amatucci, "Characteristics of the plasma impedance probe with constant bias," Physics of Plasmas, vol. 12, 2005.
3. D. D. Blackwell, D. N. Walker, S. Messer, and W. E. Amatucci, "Antenna impedance measurements in a magnetized plasma. I. Spherical antenna," Physics of Plasmas, vol. 14, 2007.
4. D. D. Blackwell, D. N. Walker, S. Messer, and W. E. Amatucci, "Antenna impedance measurements in a magnetized plasma. II. Dipole antenna," Physics of Plasmas, vol. 14, 2007.
5. D. D. Blackwell, D. N. Walker, and W. E. Amatucci, "Measurement of absolute electron density with a plasma impedance probe," Review of Scientific Instruments, vol. 76, 2005.

6. S. Clark., "Antares rocket boosts Cygnus supply ship toward International Space Station," Spaceflight Now, April 2019.
7. R. W. Freeman, R. W. James, B. Bolduc, L. A. Allen, E. Tejero, American Physical Society Division of Plasma Physics, October 2019.
8. M. H. Guerra-Mutis, C.V. Pelaez, R. C. Cabanzo, "Glow plasma jet—experimental study of a transferred atmospheric pressure glow discharge," Plasma Sources Science and Technology, vol. 12, No. 2, March 2003.
9. R. S. Harp and F. W. Crawford, "Characteristics of the Plasma Resonance Probe," Journal of Applied Physics, vol. 35, No 12, 1964.
10. I.H. Hutchinson, Principles of Plasma Diagnostics, Cambridge University Press, 1994.
11. M. D. Jensen and K. D. Baker, "Measuring ionospheric electron density using the plasma frequency probe," Journal of Spacecraft and Rockets, vol. 29, No 1, January-February 1992.
12. H. M. Jones and E. E. Kunhardt, "The influence of pressure and conductivity on the pulsed breakdown of water," I IEEE Transactions on Dielectrics and Electrical Insulation, vol. 1, No 6, December 1994.
13. B. Kay, R. W. James, R. W. Freeman, L. A. Allen, E. Tejero, "CGA Impedance Probe and CGA VSIR Sensor," Annual Directed Energy Science and Technology Symposium, West Point NY, March 2020.
14. G. D. Krebs, ThinSat 1A, space.skyrocket.de/doc_sdat/thinsat-1.htm, 1L, Hunter's Space Page, June 2019.
15. V. P. T. Ku, B. M. Annaratone, J. E. Allen, "Plasma-sheath resonances and energy absorption phenomena in capacitively coupled radio frequency plasmas. Part I," Journal of Applied Physics, vol. 84, No. 12, September 1998.
16. J. G. Laframboise, Ph.D. thesis, University of Toronto, Institute for Aerospace Studies, Report No. 100, 1966.
17. M. A. Lieberman and A. J. Lichtenberg, Principles of Plasma Discharges and Materials Processing. Wiley Interscience, New York, 1994,
18. I. V. Lisitsyn, H. Nomlyama, S. Katsuki, "Thermal processes in a streamer discharge in water," IEEE Transactions on Dielectrics and Electrical Insulation, 1999.
19. P. Nikitin and C. Swenson, "Impedance of a short dipole antenna in a cold plasma," IEEE Transactions on Antennas and Propagation , vol. 49, No. 10, October 2001.
20. H. Oya and T. Obayashi, "Measurement of Ionospheric electron density by a gyro-plasma probe: A rocket experiment by a new impedance probe," Rep. Ionos. Space Res. Jpn, 1966.
21. Shape Memory Alloy Technology Leads to Energy-Efficient CubeSat, Phys.org, phys.org/news/2019-06-memory-alloy-technology-energy-efficient-cubesat.html, University of North Texas, June 2019
22. C. T. Steigies, D. Block, M. Hirt, B. Hipp, A. Piel, and J. Grygoczuk, "Development of a fast impedance probe for absolute electron density measurements in the ionosphere," Journal of Physics D: Applied Physics, vol. 33, No. 4, February 2000.
23. D. Werner, "Will ThinSats inspire the next generation of engineers and scientists?," SpaceNews, February 2018.